# Igf1r as a therapeutic target in a mouse model of basal-like breast cancer

**Apostolos Klinakis[a], Matthias Szabolcs[b], Guoying Chen[a], Shouhong Xuan[a], Hanina Hibshoosh[b], and Argiris Efstratiadis[a,c,1]**

Departments of [a]Genetics and Development and [b]Pathology, and [c]Institute for Cancer Genetics, Columbia University, 1150 St. Nicholas Avenue, New York, NY 10032

Edited by David M. Livingston, Dana–Farber Harvard Cancer Center, Boston, MA, and approved December 5, 2008 (received for review October 11, 2008)

**Considering the strong association between dysregulated insulin-like growth factor (IGF) signaling and various human cancers, we have used an expedient combination of genetic analysis and pharmacological treatment to evaluate the potential of the type 1 IGF receptor (Igf1r) for targeted anticancer therapy in a mouse model of mammary tumorigenesis. In this particular strain of genetically modified animals, histopathologically heterogeneous invasive carcinomas exhibiting up-regulation of the *Igf1r* gene developed extremely rapidly by mammary gland-specific overexpression of constitutively active oncogenic Kras* (mutant $Kras^{G12D}$). Immunophenotyping data and expression profiling analyses showed that, except for a minor luminal component, these mouse tumors resembled basal-like human breast cancers. This is a group of aggressive tumors of poor prognosis for which there is no targeted therapy currently available, and it includes a subtype correlating with *KRAS* locus amplification. Conditional ablation of *Igf1r* in the mouse mammary epithelium increased the latency of Kras*-induced tumors very significantly (≈11-fold in comparison with the intact model), whereas treatment of tumor-bearing animals by administration of picropodophyllin (PPP), a specific Igf1r inhibitor, resulted in a dramatic decrease in tumor mass of the main forms of basal-like carcinomas. PPP also was effective against xenografts of the human basal-like cancer cell line MDA-MB-231, which carries a $KRAS^{G13D}$ mutation.**

genetically modified mouse | picropodophyllin

The IGF signaling system, which is the major determinant of mammalian organismal growth (1), has also been implicated in the pathogenesis of various human cancers (2), including breast tumors (3). A seminal observation in this regard was that cells lacking Igf1r, the tyrosine kinase receptor mediating the effects of insulin-like growth factors (IGFs), cannot be transformed by any one of several tested oncoproteins (4–6). Signaling through Igf1r does not appear to be an oncogenic component per se, but a crucial prerequisite for tumorigenesis, because among other actions, such as the promotion of cellular proliferation by stimulation of the Ras/MAPK/ERK pathway, it exerts strong PI3 kinase-dependent and independent antiapoptotic effects that are necessary for tumor growth (6). Moreover, the IGF system appears to be involved in resistance to certain anticancer regimes (7). On the basis of these considerations, potential therapeutic approaches for cancer treatment involving blocking of IGF signaling with small molecules or antibodies are currently under development (3, 6–9). In this context, we have used a 2-pronged approach to evaluate whether Igf1r is a suitable candidate for therapeutic intervention in a preclinical setting. First, based on the observation that Igf1r was overexpressed in mammary tumors advantageously induced extremely rapidly by oncogenic Kras in a mouse model, we showed genetically by breast-specific ablation of *Igf1r* expression that the cognate signal transduction pathway is causally involved in tumorigenesis in this case. This analysis provided strong justification to pursue in a second step a preclinical trial, which demonstrated favorable treatment effects of a small-molecule inhibitor of Igf1r.

## Results and Discussion

**Tumor Development in Mice Expressing Oncogenic Kras.** We have identified a suitable mouse model to evaluate Igf1r as a potential therapeutic target in the context of our research program aiming to generate mouse tumors by design using a variant of a genetic scheme involving *cre*/*loxP* recombination (10). Depending on the tissue specificity of the promoter driving *cre* expression, tumors develop at chosen anatomical sites of progeny derived by mating Cre-producers with mice carrying a dormant oncogenic transgene that becomes functional after excision of a floxed DNA segment blocking its expression.

For our purposes, we currently use the highly expressed *Eef1a1* locus (encoding a translation elongation factor) as a recipient site for transgenic knock-in of various sequences, including a constitutively active oncogenic Kras cDNA [Kras 4B(G12D); Kras*]. In our *Eef1a1*-targeting cassette (Fig. 1 *A* and *B*), 5′ and 3′ regions of *Eef1a1* gene homology are flanking a segment, eventually targeted into the first intron of the locus, which consists of a splice acceptor site, a floxed selectable marker associated with a "stop" sequence, and a cDNA (for example, Kras*) that is inserted into chosen restriction sites of a polylinker.

Ubiquitous activation of Kras* expression by removing the floxed block using a *cre* transgene transcribed in 2-cell-stage embryos (11) caused embryonic lethality (data not shown). On the other hand, crosses of Kras* mice with partners expressing Cre in particular tissues resulted in tumor development in the pancreas, prostate, skin, intestine, and the hematopoietic system (details will be presented elsewhere).

To activate expression of Kras* in mammary glands, we used a transgenic line (12) carrying *cre* inserted into the *Wap* locus, encoding a milk protein, which is specifically transcribed in alveolar and ductal mammary epithelial cells during late pregnancy and throughout lactation (13). Unexpectedly, lactating females with an *Eef1a1-Kras*/Wap*$^{cre}$ genotype ($n = 28$) developed palpable multifocal, fully invasive tumors extremely rapidly. Specifically, these malignant breast carcinomas appeared within a period of 2 days to ≈2 months after the first delivery of pups, with a median time of tumor-free survival ($T_{50}$) of only 9 days (Fig. 1*D*). This surprising observation of apparently single-step tumorigenesis can be attributed to *Kras** overexpression at a very high level (23.5 ± 5.8-fold higher than that of endogenous *Kras* mRNA, $n = 4$; see an example of Northern blot analysis in Fig. 1*C*). However, Western blot analysis indicated that the amount of total Kras (including the mutant protein form) was only moderately elevated in the neoplastic tissue in comparison with the wild type (≈4-fold; Fig. 1*C*). Whether this is caused by poor translatability or rapid turnover of the fusion Eef1a1/Kras* transcript or some other posttranscriptional mechanism remains unclear.

Author contributions: A.K. and A.E. designed research; A.K., M.S., and G.C. performed research; S.X. and H.H. contributed new reagents/analytic tools; A.K., M.S., H.H., and A.E. analyzed data; and A.K., M.S., and A.E. wrote the paper.

The authors declare no conflict of interest.

This article is a PNAS Direct Submission.

[1]To whom correspondence should be addressed. E-mail: ae4@columbia.edu.

This article contains supporting information online at www.pnas.org/cgi/content/full/0810221106/DCSupplemental.

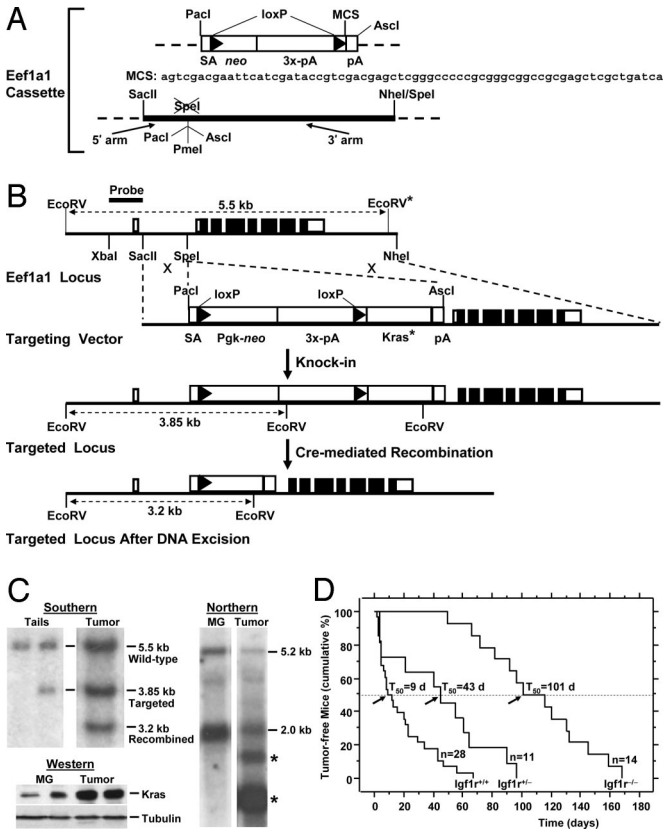


**Fig. 1.** Application of a general method for tissue-specific expression of oncoproteins in mice. (*A*) Inserts of 2 pBSK plasmids used for construction of a targeting vector for knock-in of a chosen cDNA into the *Eef1a1* locus (Eef1a1 cassette). The first plasmid consists of a splice acceptor site (0.2 kb), a floxed segment that includes a *neo* selectable marker (0.8 kb) linked to a ''stop'' sequence [3x-pA; triple poly(A); 1.5 kb], and a polylinker (multiple cloning sites; MCS), followed by an additional polyadenylation signal (pA; 0.25 kb). A chosen cDNA is cloned into the MCS, and then the entire compound insert is excised by digestion with PacI and AscI and cloned into the corresponding sites of the second plasmid that provides 5′ and 3′ homology arms to the final targeting vector. The engineered PacI and AscI sites (separated by a PmeI site) have replaced a SpeI site in the first intron of *Eef1a1*. In the work described here we have used an older version of the first plasmid, in which the *neo* gene was driven by the *Pgk* promoter (0.55 kb). (*B*) Homologous recombination in ES cells (knock-in; indicated by X symbols) using a targeting vector that was constructed by inserting an oncogenic Kras cDNA (Kras*; 1.1 kb; see *Materials and Methods*) into the MCS of the Eef1a1 cassette. A simplified restriction map and the noncoding and coding exons of the locus (open and filled rectangles, respectively) are indicated. Excision of the floxed block from the targeted allele by Cre-mediated recombination (using in this case a Wap-cre transgene for specific expression of the recombinase in mammary glands) allows Kras* transcription driven by the *Eef1a* promoter. (*C*) Molecular analyses. Southern blot analysis was performed by using EcoRV-digested DNA that was extracted from tails or Kras*-induced tumors. Northern blot analysis shows that in addition to the 2 endogenous Kras mRNAs transcribed from the intact allele in wild-type mammary glands (MG), 2 new Kras* transcripts (asterisks) are expressed from the targeted allele in tumors. Western blot analysis using an antibody recognizing the Kras4B isoform encoded by Kras* indicates that the amount of the oncoprotein is significantly higher in mammary tumors than in normal glands. (*D*) Kaplan–Meier tumor-free mouse survival curves. The survival of female mice from the day of the first parturition until the day of detection of palpable Kras*-induced tumors is compared between animals carrying the oncogenic transgene either in the presence of wild-type *Igf1r* or in a genetic background in which one or both floxed *Igf1r* alleles have been conditionally ablated. In mice possessing at least 1 intact *Igf1r* allele, tumors appear immediately after a single pregnancy, in contrast to the animals with *Igf1r* nullizygous mammary epithelial cells (3 pregnancies).

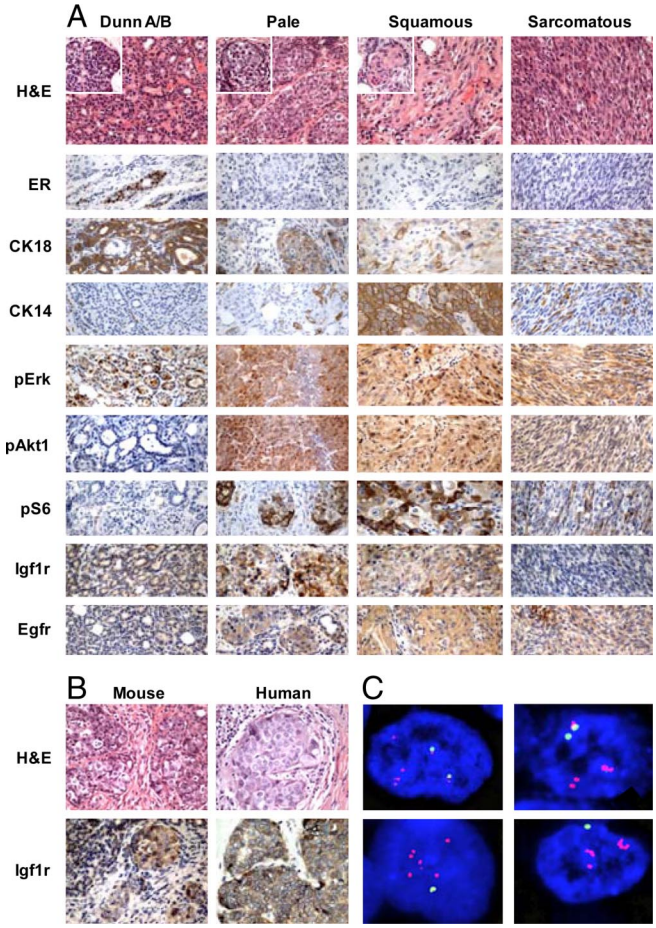


**Fig. 2.** Histology and immunophenotyping of mammary carcinomas. (*A*) Kras*-induced mouse mammary tumors exhibit 4 histopathological forms. The insets in the H&E-stained sections in the top row show CISs of the corresponding invasive carcinomas. For details about the immunostaining results, see text and Table S2. (*B*) Examples of mouse and human pale breast cancers. A mouse Kras*-induced pale cell carcinoma exhibits a strong histological similarity (H&E staining) with a specimen of human atypical medullary breast cancer, and both tumor types are strongly positive for Igf1r immunostaining. (*C*) *KRAS* copy gains in some atypical medullary breast cancers with pale cells. The dual-color FISH analysis using *KRAS* (red) and chromosome 12 centromeric (green) probes shows that in cells from 3 different human pale breast cancer specimens (the right panels are from the same tumor), there are copy gains of the 12p12.1 region (up to 6 KRAS copies). (Magnification: *A*, *A Insets*, *B*, 400×; *C*, 1,000×.)

**Histopathological Analysis of Kras*-Induced Mammary Carcinomas.** Female mice developing tumors were killed when moribund within a period of 9 days to ≈3 months (this brief time of observation only rarely permitted the detection of lung metastases). In all examined cases ($n = 37$), the Kras*-induced carcinomas involved most or all mammary glands and were either multifocal or consisted of large masses generated by coalescence of smaller components. The tumors were histologically heterogeneous, and 4 coexistent types of invasive carcinomas were identified at variable proportions: adenocarcinomas (Dunn type A/B tumors), and pale (PCC), squamous (SCC), and spindle cell (sarcomatous: SRC) carcinomas [Fig. 2*A*; the features of cancer forms are summarized in supporting information (SI) Table S1].

The Dunn adenocarcinomas were well-differentiated microacinar structures (Dunn type A) or occasionally solid nests without glandular differentiation (Dunn type B) and corresponded morphologically to tumor types induced by the mouse mammary tumor virus (14, 15). On average, they were the smallest and slowest-

growing tumor constituents (Table S1). The PCCs, which consisted of large, lightly staining ("pale") cells, were also adenocarcinomas, but exhibited in some areas signs of keratinization. Clear evidence of keratinization (squamous metaplasia) was seen in SCC, whereas the spindle cell tumors exhibited sarcomatous metaplasia. The microacinar (Dunn A), pale, and squamous cell tumors were correlated with the presence of corresponding forms of carcinoma in situ (CIS; also referred to in mice as *mammary intraepithelial neoplasm*; Fig. 2*A Insets*) (16). Because the squamous CIS was rarely observed, we surmise that it gives rise to invasive SCC very rapidly. A distinct spindle cell CIS was not found, but occasionally squamous CIS exhibiting foci of sarcomatous metaplasia could be recognized.

To assess the origin, relationships, and signaling characteristics of the carcinomas by immunophenotyping, we used an extensive panel of markers (Fig. 2*A*; see also Fig. S1 and Table S2). The results indicated that the $ER^+/PR^+$ Dunn adenocarcinomas, which express exclusively luminal cell markers, such as cytokeratin 18 (CK18; Krt18), are luminal-type cancers, presumably derived from differentiated luminal epithelial cells. In contrast, on the basis of their distinct features, the pale, squamous, and sarcomatous carcinomas appear to correspond to basal-like breast carcinomas.

Of the 3 major molecularly classified subtypes of human breast cancer (17–19), luminal cancers are estrogen receptor-positive ($ER^+$), whereas the other 2 classes are ER-negative and either overexpress ERBB2 ($ERBB2^+$) or exhibit phenotypic features of basal/myoepithelial cells (basal-like cancers). The latter also lack progesterone receptor (PR) and ERBB2 ("triple negative breast cancers"; see refs. 20 and 21) but frequently express EGFR and basal markers, such as cytokeratins (CKs) 5/6 and/or 14 and p63 (22). The basal-like group (15–20% of all breast cancers), which is quite heterogeneous, includes high proportions of BRCA1-associated and also medullary and metaplastic (squamous, spindle cell, and other) subtypes. Interestingly, KRAS amplification was detected in 56% (9/16) of examined basal-like human breast cancers (23).

We propose that the Kras*-induced $ER^-/PR^-$ pale, squamous, and sarcomatous mouse carcinomas, which are immunopositive for both luminal (CK18) and basal (CK5, CK14, p63 and, rarely, smooth muscle actin) cell markers, and also for presumptive stem cell markers (Table S2), are analogous to some of the forms of human basal-like cancers. It is likely that these basal-like murine tumors are derived from undifferentiated, bipotential precursor cells and not from myoepithelial cells (this hypothesis concerning "cells of origin" is discussed in detail in the *SI Text*). Consistent with this view is the fact that the *Kras** activating *cre* is embedded in the *Wap* locus that is not expressed in fully differentiated myopithelial cells.

Interestingly, we noted a morphological similarity between mouse PCC and a type of human basal-like breast cancer that was also correlated with KRAS copy gain. In a collection of human breast cancer specimens ($n = 94$), 17 samples (18%) were found to be basal-like (triple-negative and positive for CK5/6), whereas 77 (82%) were nonbasal (R. Parsons and H.H., unpublished data). Analysis of the 17 basal cancers for amplification of the KRAS locus by using CGH showed that 5 of the specimens scored positive, whereas further analysis of a subset by using FISH identified a sixth positive sample. The corresponding KRAS amplification frequency in the nonbasal samples detected by CGH was 4/77 [≈5% vs. ≈35% (6/17) $P = 0.002$, Fisher exact test]. Three of the basal-like specimens with amplified KRAS displayed medullary features (large tumor nodules with pushing rather than infiltrative borders, composed of large cells with irregular, sometimes bizarre nuclei growing in a syncytial fashion), but none of them met all of the criteria for classical medullary carcinoma classification [they are referred to here as *atypical medullary breast cancer* (AMBC); ref. 24]. Interestingly, 2 of these AMBCs contained abundant large cells with pale or clear cytoplasm and exhibited a strong resemblance to the histomorphological signature of the PCC observed in our mouse model. To validate this correlation, we examined an available set of triple-negative AMBCs ($n = 8$) and observed that most of them (7/8) were at least focally comparable to the PCC in Kras* mice (Fig. 2*B*). Immunohistochemical analysis showed that all 8 of these AMBCs were positive for basal CKs 5 and 14 and showed IGF1R staining along their cellular surface (Fig. 2*B*). We then performed FISH analysis to assess potential amplification of the *KRAS* locus and found that 3 of these cancers, all of which possessed large pale cells as a major component, tested positive ($P = 0.015$, using the data 3/8 for basal and 4/77 for nonbasal specimens; Fig. 2*C*). We conclude, therefore, that a subset of basal-like human breast cancers preferentially exhibit amplification of the *KRAS* locus frequently associated with a PCC character.

**Molecular Analysis of Kras*-Induced Mammary Carcinomas.** To complement the morphological analysis, we examined the expression profiles of normal postinvolutional mammary glands ($n = 5$) and Kras*-induced carcinomas ($n = 14$), and found that they were readily discriminated by unsupervised hierarchical clustering (Fig. S2). Although the dendrogram also stratified the tumors according to the predominating basal-like component, we used for comparison only average differential expression levels in tumors vs. normal glands to simplify our analysis (the microarray data were validated in part by immunohistochemistry and Northern or Western blotting).

Comparisons of our profiling results with lists of basal and luminal markers chosen for classification of human breast cancers (23, 25) and also with datasets of up-regulated and down-regulated genes in basal and nonbasal breast cancers (26, 27) showed unequivocally that the Kras*-induced tumors are basal-like carcinomas, in agreement with the histological evidence. In fact, the null hypothesis that there is no statistical difference in the representation of basal and luminal markers in the groups of up-regulated and down-regulated genes in Kras* tumors was overwhelmingly rejected (Table S3). In addition, consistent with the hypothesis that the basal-like Kras* cancers evolve from precursor cells of the mammary epithelium, the data showed that the pattern of overexpressed genes in the tumors resembled much more the profile of a mammary cell population enriched in stem cells than that of another population consisting predominantly of luminal cells (Table S3) (28). Not unexpectedly, there was a high degree of similarity between the profiles of Kras*-induced mouse lung (29) and mammary tumors (Table S3). Finally, comparisons of the microarray results with those for other mouse mammary tumors supported strongly the view that Kras* deregulates to a much larger extent all major signaling pathways (Tables S4–S6).

We note that several genes previously discussed in the context of Kras*-induced neoplastic lesions of the lung (29) or the pancreas (30), such as *Ccnd1* (cyclin D1), *Dusp6*, *Phlda1*, and *Ptgs2* (Cox2), were also up-regulated in the mammary carcinomas that we analyzed. An additional observation that was crucial for the focus of our work was the increased expression of the *Igf1r* gene that was confirmed by Northern blot analysis (steady-state level ≈3-fold over normal; data not shown).

**Conditional Ablation of *Igf1r* Delays Kras*-Induced Mammary Tumorigenesis.** To examine the impact of the absence of Igf1r on the development of Kras*-induced mammary carcinomas, we compared tumor progression between animals carrying the oncogenic transgene in a background either wild type for *Igf1r* (Eef1a1-Kras*/$Wap^{cre}$ mice serving as controls) or possessing 1 or 2 floxed *Igf1r* alleles that could be conditionally ablated (Eef1a1-Kras*/$Wap^{cre}$/$Igf1r^{fl/+}$ and Eef1a1-Kras*/$Wap^{cre}$/$Igf1r^{fl/fl}$ genotypes; $n = 11$ and $n = 14$, respectively).

We observed that in contrast to cancer manifestation after the first birth with a $T_{50}$ of 9 days in control mice, ablation of both floxed *Igf1r* alleles in experimental animals resulted in tumor development only after 3 pregnancies, whereas the latency increased dramatically

(11-fold; $T_{50}$ = 101 days; $P < 0.0001$, log-rank test; Fig. 1*D*). However, complete rescue was not observed, perhaps owing to the occurrence of mutational and/or epigenetic alterations compensating for the absence of IGF signaling (Southern blot analysis confirmed that Cre-mediated recombination had occurred in the *Igf1r* locus, whereas the tumors lacked Igf1r expression detectable by immunohistochemistry or by Northern/Western blot analysis; data not shown). Immunostaining for all examined markers (including pAkt, pErk1/2, and pS6) was virtually unaltered in the $Igf1r^{-/-}$ tumors, whereas significant differences in the multifocality and overall size of the carcinomas or in the proliferation indices of the components were not noted (Table S1). On the other hand, with the exception of SRC, significant alterations were observed in the relative sizes of the components (Table S1). Interestingly, the absence of only 1 *Igf1r* allele (Eef1a1-Kras*/$Wap^{cre}$/$Igf1r^{fl/+}$ animals) also resulted in a statistically significant delay in tumor appearance after a first pregnancy (≈5-fold increase in latency; $P = 0.01$; Fig. 1*D*).

Comparison of the expression profiles of Kras* cancers developing in the presence or absence of Igf1r signaling revealed, among other effects (Table S5), significant differences in transcript levels for Egf ligands that were confirmed by Northern blot analysis. Specifically, with intact Igf1r there was >100-fold increase over normal in the amount of steady-state mRNA for Hbegf present in the tumors, whereas the levels of overexpressed transcripts for Areg, Ereg, and Tgfa were less dramatic (≈4-, 15-, and 6-fold, respectively). Interestingly, a similar overexpression of Egf ligands was observed in an $Hras^{G12V}$ breast cancer model (31), implying a more general feedback loop involving Ras protein function. We found that elimination of Igf1r only slightly affected the overexpression of *Areg*, but resulted in the reduction of the *Ereg* and *Tgfa* transcripts to almost normal levels, whereas the previously enormous amount of *Hbegf* mRNA was reduced approximately by half. In contrast, *Igf1* and *Igf2* transcripts encoding IGF ligands were virtually absent from the tumors, and Igf1 and Igf2 polypeptides were below detection limits by immunohistochemistry (Table S2), indicating absence of IGF autocrine/paracrine signaling cues. Accordingly, unless it is eventually found that Igf1r-mediated signaling is triggered by EGF ligands acting through noncanonical IGF1R–EGFR heterodimers (32), it is likely that the IGF functions are served in the Kras* mammary cancers by endocrine action of IGF1 circulating in serum. Assuming this to be the case, it appears that IGF signaling potentiates Erbb-mediated activities by up-regulating Egf ligands through an unknown mechanism, which could be transcriptional and could involve Ap1 sites present in the promoter regions of some of these ligands (33). Interestingly, Fosl1, an Ap1 component, is highly overexpressed in the Kras* tumors (Fig. S1 and Table S2). Three of the four Erbb receptors (Egfr, Erbb2, and Erbb3) are present in the Kras* tumors, but they are not overexpressed. In fact, Erbb2 transcripts remain undetectable by Northern blot analysis, although the receptor itself can be seen in the carcinomas by immunostaining (Fig. S1).

**Table 1. Drug treatments**

| | Mice, *n* | Glands, *n* | Tumor volume per gland, $mm^3$† | Percent | *P*‡ |
|---|---|---|---|---|---|
| Mouse tumors | | | | | |
| Vehicle | 7 | 21 | 217.8 ± 65.6 | 100 | |
| Erlotinib | 4 | 16 | 66.9 ± 29.3 | 30.7 | 0.005 |
| PPP | 5 | 17 | 16.0 ± 9.1 | 7.3 | <0.001 |
| PPP + Erlotinib | 5 | 18 | 8.6 ± 3.9 | 3.9 | <0.0001 |
| Xenografts | | | | | |
| Vehicle | 5 | 20 | 304 ± 40.8 | 100 | |
| PPP | 5 | 20 | 215 ± 18.6 | 70.7 | 0.02 |

†Values are mean ± SEM.

‡Because of data skewness, in tumor volume comparisons between the drug treatments and the control (vehicle), probabilities (*P*) were calculated by using Student's *t* test after logarithmic transformation of the values to meet the distribution criterion of the test.

**Pharmacological Treatment of Kras*-Induced Mammary Tumors.** Our genetic evidence for an Igf1r role in mammary tumorigenesis, at least in the examined model, is significant in the context of efforts to develop therapeutic approaches for treating breast cancer by blocking IGF signaling. This could turn out to be significant for basal-like carcinomas, which have poor prognosis (18) and pose a serious problem to targeted therapies (34, 35), considering that the use of antiestrogens in combination with trastuzumab (anti-ERBB2 antibody) is not an option, whereas there is no clear choice for chemotherapy. We decided, therefore, to use the Kras* model in a preclinical study testing the efficacy of the cyclolignan picropodophyllin (PPP), which has recently emerged as a potent, nontoxic, and highly specific Igf1r inhibitor (36). Although the molecular mechanism of PPP action is still unknown, its inhibitory effects appear to be exerted by abrogation of Igf1r phosphorylation and promotion of its degradation, whereas the homologous insulin receptor is not affected (36, 37). Cell lines of Igf1r null fibroblasts are apparently insensitive to PPP, whereas the drug reduces the viability of cancer cell lines and causes tumor regression in mouse xenografts of multiple myeloma (38) and uveal melanoma (39). We tested, therefore, the potential therapeutic effects of PPP on breast cancer using the Kras* model by administering the drug either alone or in combination with erlotinib, an Egfr inhibitor (40), taking into consideration the overexpression of Erbb ligands described above.

Mice at a progressed stage of tumorigenesis bearing at least 1 readily palpable tumor were injected i.p. once daily either with vehicle or with PPP and erlotinib, alone or in combination, at doses of 30 mg/kg and 50 mg/kg, respectively, for a period of 3 weeks, taking into account that the weight of some tumors in the controls could reach or exceed ≈1 g by that time. At the end of treatment, we measured tumor growth relative to control values by calculating tumor mass, and we did not attempt sequential measurements using a caliper because a pilot study indicated that they were inaccurate. First, the tumors developing in each gland tended to be multifocal and uneven, and they progressively coalesced into larger masses precluding reliable evaluation. In addition, the treatment resulted in extensive tumor necrosis and fibrosis detectable only histologically, which would have artificially inflated macroscopic measurements.

We analyzed all glands carrying tumors in treated and control animals, and for statistical evaluation we took into account that the cancers exhibited pronounced size heterogeneity. On average, either erlotinib or PPP was effective and did not permit expansion of tumor volume per mammary gland beyond levels of ≈30% and ≈7% of the control value, respectively (Table 1). The effect of the drugs used in combination (≈4% of control) was perhaps only additive (dose–response relationships were not yet studied). Monitoring of body weights and histological examination of various organs from vehicle- and drug-treated mice did not reveal signs of nonspecific toxicity.

Not unexpectedly, vehicle administration did not alter the histopathological or immunophenotypic profile of tumors, whereas the specimens of mice treated either with PPP or with a PPP/erlotinib combination displayed a marked reduction in or even an absence of the pale and squamous cell components accompanied by extensive keratinization and vacuolation (Fig. 3). Thus, small cancerous lesions observed after treatment consisted only of glandular and spindle cell types. The extent of the latter, however, which exhibited degenerative changes, is difficult to quantitate. Erlotinib acting alone reduced predominantly the pale cell component. However, residual squamous cell carcinomas, whenever encountered together with glandular and spindle cell components, exhibited extensive degenerative changes and marked tumor necrosis.

To ascertain whether the reduction in tumor volume was a

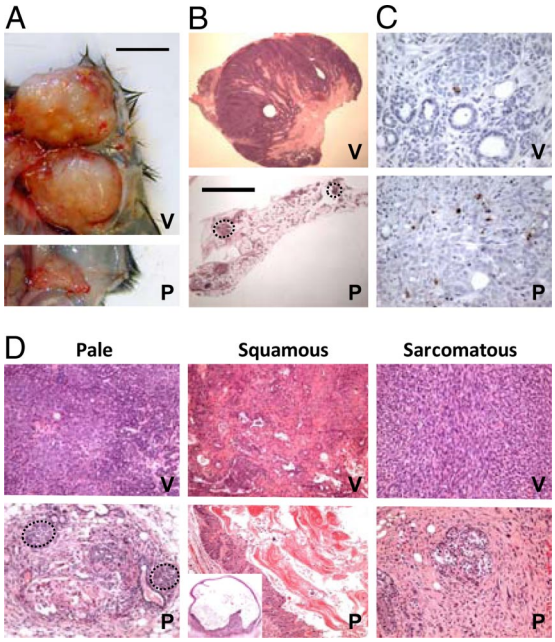


**Fig. 3.** Drug treatment of Kras*-induced mammary carcinomas. (*A*) Examples of gross anatomical examination of tumors that developed in mice carrying an activated Kras* oncogenic transgene after 3 weeks of treatment either with vehicle (V) or with picropodophyllin (P). (*B*) Histological examination of the tumors shows that in comparison with the controls (V), the PPP-treated tumors are dramatically smaller (P; dotted circles). (*C*) Compared with vehicle injections (V), administration of PPP for 3 days (P) increases ≈9-fold the level of apoptosis detected in the pale component, as assayed by activated caspase 3 immunohistochemistry (brown staining; for details see text). (*D*) Comparison of the effects on the components of Kras*-induced carcinomas between PPP administration (P) and vehicle injections (V) for 3 weeks. The PPP treatment diminishes the size of pale cell tumors (dotted circles) and results in extensive keratinization and vacuolation (*Inset*) of the squamous component. The sarcomatous component remaining after treatment might be overestimated, because it exhibits variable degrees of degenerate changes that are difficult to quantitate, including replacement fibrosis (increased matrix and collagen deposition and proliferation of Fosl1-negative myofibroblasts). (Scale bar, 0.5 cm.) (Magnification: *C*, *D*, 400×; *C Inset*, *D Inset*, 100×.)

consequence of decreased proliferation or increased cell death, we determined proliferation indices, and as a measure of apoptosis examined the expression of activated caspase-3 after only 3 days of PPP or PPP plus erlotinib treatment; that is, before a drastic decrease of the pale and squamous cell components. We observed that although proliferation was still at control levels, the numbers of caspase-3-positive cells in the microacinar and nonglandular components were 2- and 9-fold higher, respectively, than in controls (Fig. 3*C*).

To evaluate IGF1R as a drug target in human cells, we targeted the receptor in MDA-MB-231 mammary cancer cells, which possess a $Kras^{G13D}$ mutant gene (41, 42) and share similarities in transcriptional profile with the basal-like mammary tumor cell line (43). Pharmacological inhibition using PPP drastically reduced the in vitro viability of MDA-MB-231 cells (Fig. S3*A*). In addition, IGF1R knockdown using either a dominant-negative form of the receptor or siRNA had an analogous effect (Fig. S3 *B* and *C*). In a xenograft model in NOD/SCID mice, we showed that tumor growth from orthotopically injected MDA-MB-231 cells was also attenuated in PPP-treated mice in comparison with vehicle-treated controls (Table 1). Although the in vivo effect of PPP on the highly invasive MDA-MB-231 xenografts was overall less pronounced than that observed with the mouse carcinomas, it was statistically significant. In addition to other factors, such as poor vascularization making the drug less accessible, the behavior of these xenografts derived from MDA-MB-231 cells that are more spindly than epithelial may be analogous to the relatively reduced response of the SRC component of mouse Kras* tumors to PPP. Nevertheless, in conjunction with the mouse data, these observations provide strong justification for further evaluations of the drug against human breast cancer.

**Concluding Remarks.** We have shown that overexpression of oncogenic Kras* in mouse mammary glands leads to rapid development of histopathologically heterogeneous malignant tumors predominantly simulating human basal-like breast cancers, but also including a luminal type. Although the incidence of *KRAS* mutations in human breast cancer is not very high, it is still appreciable (≈7% in tumors and ≈13% in cancer cell lines; see refs. 42 and 44). Moreover, in ≈70% of primary breast cancers, the level of RAS is higher than that in normal tissue (45). Such elevated RAS activity is apparently required even for mammary carcinogenesis induced by *RAS* mutations (31). Clearly, regardless of cause (mutation and/or overexpression), the important element contributing to oncogenesis is the perturbation of the Ras pathway, which can be dissected genetically by mouse modeling. The diversity of cancerous forms, and especially the rapidity of tumor manifestation, increases further the utility of the mouse model that we have described here, which can be used advantageously after appropriate genetic testing for preclinical evaluation of treatment regimes, as exemplified by our results.

Seemingly, the single-step tumorigenesis that we have observed does not conform to the widely accepted multihit model of carcinogenesis (46, 47). However, from the standpoint that cancer is a disease of malfunctioning cell signaling, all cases of tumor development can be viewed, regardless of timing, as variants of a more general hypothesis positing that contributing "hits" correspond to recruitment and combinatorial engagement of deregulated pathways predominantly involved in apoptosis and growth control. Apparently, in the case of our model, highly overexpressed, constitutively active Kras* can elicit synergism of downstream pathways that are simultaneously deregulated to a degree sufficient for rapid development of invasive cancer. We have observed analogous inverse reciprocity between Kras* expression levels and tumor latency in other mouse models (A.K. and A.E., unpublished data) and note that extremely rapid development of carcinomas of the skin and the oral mucosa also induced by Kras* was observed by others (48). It remains to be seen whether, by exceeding normally affordable limits, oncogene overexpression overrides homeostatic capabilities and/or whether the excessive deregulation that it causes permits novel and abnormal signaling interactions.

An additional open question is why the constitutively acting oncogenic Kras*, which has ceased to respond to upstream effectors in signaling relays and has presumably acquired autonomy in deregulating signaling, is not refractory to the silencing of Igf1r. Ras proteins control proliferation through the Raf→MEK→Erk pathway but also interact directly with the p110 catalytic subunit of the PI3K complex, thus affecting antiapoptosis. It is notable, in this regard, that loss-of-function missense mutations in the Ras-binding domain of p110 inhibit almost completely Kras and Hras oncogenicity in mouse models of lung and skin tumors, respectively (49). The mechanistic details in our case (involving a different tissue) are unclear. However, we hypothesize that without the crucial participation of Igf1r signaling that exerts both PI3K-dependent and PI3K-independent antiapoptotic effects, the direct activation of the PI3K pathway by Kras* is, despite its overexpression, inadequate for attaining a level of antiapoptosis able to promote oncogenicity. We note that the results of a previous study (50) showing that 32D cells could become tumorigenic by the combined action of Hras and Irs1 (a downstream effector of Igf1r), but not by either one of these components acting alone, could also be interpreted as indicating a collaboration between the Erk and PI3K pathways. Perhaps, among other effects, Kras* triggers in our case the operation of a positive feedback loop that enhances its action through the up-regulation of Igf1r expression which, in turn, could amplify proliferative and

antiapoptotic signaling by increasing the expression of Egf ligands. The down-regulation of such ligands by genetic inactivation of Igf1r could explain why PPP is more effective than erlotinib in the treatment of Kras*-induced tumors. Presumably, pharmacological inhibition of Egfr alone does not attenuate tumor growth sufficiently, because the Egf ligands are still expressed at high levels and can function through other receptors of the family (the most likely candidates are Erbb2:Erbb3 heterodimers). In contrast, in addition to the direct pharmacological inhibition of Igf1r activity by PPP, there is an indirect effect on Egf ligand down-regulation preventing the robust formation of homodimers or heterodimers between the Erbb receptor family members.

Although elucidation of mechanistic details will be a slow and painstaking process, a testable hypothesis directly related to the general view of collaborating tumorigenic pathways is that regardless of their exact identity, number, and mode of engagement (simultaneous or sequential), each one of them is indispensable for malignancy, and that blocking any step in any of the signaling cascades by pharmacological intervention would at least ameliorate the oncogenic process. Successful combination regimens will be, of course, even more suitable for therapy.

## Materials and Methods

**Mice.** In addition to the mice conditionally expressing oncogenic Kras (for details, see *SI Text*), we used 3 mouse strains that we have described previously: 2 *cre*-expressing strains, Hs-cre1 and Wap$^{cre/+}$ (11, 12), and *Igf1r*$^{flox/flox}$ mice (11). Molecular, histological, microarray, and other analyses were performed as described in *SI Text* and Table S7.

**Drug Treatments.** Details of the preclinical trial using PPP synthesized as described (51) and erlotinib (purchased from Hwasun Biotechnology Co.) are described in *Results*. The drugs were dissolved in DMSO and cremophor (9:1) and injected i.p. To calculate tumor volumes, we used the formula for a prolate spheroid ($\pi/6 \times a \times b^2$ or $\approx a \times b^2/2$, where $a$ and $b$ are the major and minor axis, respectively). The lengths of axes were determined microscopically from sections of tumor nodules using a computer-assisted morphometry system (SpotAdvanced VS. 4.0.1; Nikon Eclipse E400). For xenograft experiments, $5 \times 10^6$ MDA-MB-231 cells were injected bilaterally into the fat pads of mammary glands 3 and 4 of female NOD/SCID mice. At 10 days after injection, when tumors were readily palpable, the mice were randomly divided into 2 groups of 5 mice each and received the same treatment (vehicle or PPP) described above for the Kras* mice for 3 weeks. For in vitro experiments, MDA-MB-231 cells were grown in DMEM supplemented with 10% FBS. Equal numbers of cells were seeded in multiple wells of 24-well plates at low density (≤20% confluence at day 0), and either DMSO or PPP dissolved in DMSO was added to the medium (final concentrations: DMSO 0.1% and PPP 500 nM). Cell viability (duplicates) was measured on days 2, 4, and 6 by using the Thiazolyl Blue Tetrazolium Bromide (MTT) colorimetric assay (52).

**SI.** Additional information and results can be found in *SI Text* and Figs. S4 and S5.

**ACKNOWLEDGMENTS.** We thank Joe Terwilliger for advice on statistical analysis; Ramon Parsons for communicating unpublished information; Renato Baserga, Tyler Jacks, Vincent L. Morris, Arch Perkins, David Tuveson, and Louis E. Underwood for materials; Monica Mendelsohn for help in generating transgenic mice; Zhe Li and Yonghui Zhang for help with microarray analysis; Vundavalli Murty for FISH; and Qiong Li and Xi Sun for expert technical assistance. This work was supported by National Cancer Institute Grant 1 P01 CA97403 (Project 2) (to A.E.) and by a gift from the Berrie Foundation. A.K. was supported by a Fellowship from the Jane Coffin Childs Memorial Fund for Medical Research.

1. Efstratiadis A (1998) Genetics of mouse growth. *Int J Dev Biol* 42:955–976.
2. Pollak MN, Schernhammer ES, Hankinson SE (2004) Insulin-like growth factors and neoplasia. *Nat Rev Cancer* 4:505–518.
3. Sachdev D, Yee D (2006) Inhibitors of insulin-like growth factor signaling: a therapeutic approach for breast cancer. *J Mammary Gland Biol Neoplasia* 11:27–39.
4. Sell C, *et al.* (1993) Simian virus 40 large tumor antigen is unable to transform mouse embryonic fibroblasts lacking type 1 insulin-like growth factor receptor. *Proc Natl Acad Sci USA* 90:11217–11221.
5. Sell C, *et al.* (1994) Effect of a null mutation of the insulin-like growth factor I receptor gene on growth and transformation of mouse embryo fibroblasts. *Mol Cell Biol* 14:3604–3612.
6. Baserga R (2005) The insulin-like growth factor-I receptor as a target for cancer therapy. *Expert Opin Ther Targets* 9:753–768.
7. Ryan PD, Goss PE (2008) The emerging role of the insulin-like growth factor pathway as a therapeutic target in cancer. *Oncologist* 13:16–24.
8. Garcia-Echeverria C (2006) Medicinal chemistry approaches to target the kinase activity of IGF-1R. *IDrugs* 9:415–419.
9. Hartog H, Wesseling J, Boezen HM, van der Graaf WT (2007) The insulin-like growth factor 1 receptor in cancer: Old focus, new future. *Eur J Cancer* 43:1895–1904.
10. Politi K, *et al.* (2004) 'Designer' tumors in mice. *Oncogene* 23:1558–1565.
11. Dietrich P, Dragatsis I, Xuan S, Zeitlin S, Efstratiadis A (2000) Conditional mutagenesis in mice with heat shock promoter-driven cre transgenes. *Mamm Genome* 11:196–205.
12. Ludwig T, Fisher P, Murty V, Efstratiadis A (2001) Development of mammary adenocarcinomas by tissue-specific knockout of Brca2 in mice. *Oncogene* 20:3937–3948.
13. Robinson GW, McKnight RA, Smith GH, Hennighausen L (1995) Mammary epithelial cells undergo secretory differentiation in cycling virgins but require pregnancy for the establishment of terminal differentiation. *Development* 121:2079–2090.
14. Dunn TB (1959) in *The Physiopathology of Cancer*, ed Homburger F (Hoeber-Harper, New York), pp 38–84.
15. Sass B, Dunn TB (1979) Classification of mouse mammary tumors in Dunn's miscellaneous group including recently reported types. *J Natl Cancer Inst* 62:1287–1293.
16. Cardiff RD, Munn RJ, Galvez JJ (2007) in *The Mouse in Biomed Res Volume II: Diseases*, eds Fox JG, *et al.* (Elsevier, New York), 2nd Ed, pp 581–622.
17. Perou CM, *et al.* (2000) Molecular portraits of human breast tumours. *Nature* 406:747–752.
18. Sorlie T, *et al.* (2001) Gene expression patterns of breast carcinomas distinguish tumor subclasses with clinical implications. *Proc Natl Acad Sci USA* 98:10869–10874.
19. Sorlie T, *et al.* (2003) Repeated observation of breast tumor subtypes in independent gene expression data sets. *Proc Natl Acad Sci USA* 100:8418–8423.
20. Da Silva L, Clarke C, Lakhani SR (2007) Demystifying basal-like breast carcinomas. *J Clin Pathol* 60:1328–1332.
21. Reis-Filho JS, Tutt AN (2008) Triple negative tumours: A critical review. *Histopathology* 52:108–118.
22. Nielsen TO, *et al.* (2004) Immunohistochemical and clinical characterization of the basal-like subtype of invasive breast carcinoma. *Clin Cancer Res* 10:5367–5374.
23. Herschkowitz J, *et al.* (2007) Identification of conserved gene expression features between murine mammary carcinoma models and human breast tumors. *Genome Biol* 8:R76.
24. Fadare O, Tavassoli FA (2007) The phenotypic spectrum of basal-like breast cancers: A critical appraisal. *Adv Anat Pathol* 14:358–373.
25. Sorlie T, *et al.* (2006) Distinct molecular mechanisms underlying clinically relevant subtypes of breast cancer: Gene expression analyses across three different platforms. *BMC Genomics* 7:127.
26. Farmer P, *et al.* (2005) Identification of molecular apocrine breast tumours by microarray analysis. *Oncogene* 24:4660–4671.
27. Richardson AL, *et al.* (2006) X chromosomal abnormalities in basal-like human breast cancer. *Cancer Cell* 9:121–132.
28. Stingl J, *et al.* (2006) Purification and unique properties of mammary epithelial stem cells. *Nature* 439:993–997.
29. Sweet-Cordero A, *et al.* (2005) An oncogenic KRAS2 expression signature identified by cross-species gene-expression analysis. *Nat Genet* 37:48–55.
30. Hingorani SR, *et al.* (2003) Preinvasive and invasive ductal pancreatic cancer and its early detection in the mouse. *Cancer Cell* 4:437–450.
31. Sarkisian CJ, *et al.* (2007) Dose-dependent oncogene-induced senescence in vivo and its evasion during mammary tumorigenesis. *Nat Cell Biol* 9:493–505.
32. Riedemann J, Takiguchi M, Sohail M, Macaulay VM (2007) The EGF receptor interacts with the type 1 IGF receptor and regulates its stability. *Biochem Biophys Res Commun* 355:707–714.
33. Ornskov D, Nexo E, Sorensen BS (2007) Insulin induces a transcriptional activation of epiregulin, HB-EGF and amphiregulin, by a PI3K-dependent mechanism: Identification of a specific insulin-responsive promoter element. *Biochem Biophys Res Commun* 354:885–891.
34. Cleator S, Heller W, Coombes RC (2007) Triple-negative breast cancer: Therapeutic options. *Lancet Oncol* 8:235–244.
35. Carey LA, *et al.* (2007) The triple negative paradox: Primary tumor chemosensitivity of breast cancer subtypes. *Clin Cancer Res* 13:2329–2334.
36. Girnita A, *et al.* (2004) Cyclolignans as inhibitors of the insulin-like growth factor-1 receptor and malignant cell growth. *Cancer Res* 64:236–242.
37. Vasilcanu R, *et al.* (2008) Picropodophyllin induces downregulation of the insulin-like growth factor 1 receptor: Potential mechanistic involvement of Mdm2 and beta-arrestin1. *Oncogene* 27:1629–1638.
38. Menu E, *et al.* (2007) Targeting the IGF-1R using picropodophyllin in the therapeutical 5T2MM mouse model of multiple myeloma: Beneficial effects on tumor growth, angiogenesis, bone disease and survival. *Int J Cancer* 121:1857–1861.
39. Girnita A, *et al.* (2006) The insulin-like growth factor-I receptor inhibitor picropodophyllin causes tumor regression and attenuates mechanisms involved in invasion of uveal melanoma cells. *Clin Cancer Res* 12:1383–1391.
40. Yang SX, Simon RM, Tan AR, Nguyen D, Swain SM (2005) Gene expression patterns and profile changes pre- and post-erlotinib treatment in patients with metastatic breast cancer. *Clin Cancer Res* 11:6226–6232.
41. Kozma SC, *et al.* (1987) The human c-Kirsten ras gene is activated by a novel mutation in codon 13 in the breast carcinoma cell line MDA-MB231. *Nucleic Acids Res* 15:5963–5971.
42. Hollestelle A, Elstrodt F, Nagel JH, Kallemeijn WW, Schutte M (2007) Phosphatidylinositol-3-OH kinase or RAS pathway mutations in human breast cancer cell lines. *Mol Cancer Res* 5:195–201.
43. Charafe-Jauffret E, *et al.* (2006) Gene expression profiling of breast cell lines identifies potential new basal markers. *Oncogene* 25:2273–2284.
44. Malaney S, Daly RJ (2001) The ras signaling pathway in mammary tumorigenesis and metastasis. *J Mammary Gland Biol Neoplasia* 6:101–113.
45. Dati C, *et al.* (1991) c-erbB-2 and ras expression levels in breast cancer are correlated and show a co-operative association with unfavorable clinical outcome. *Int J Cancer* 47:833–838.
46. Vogelstein B, Kinzler KW (1993) The multistep nature of cancer. *Trends Genet* 9:138–141.
47. Hanahan D, Weinberg RA (2000) The hallmarks of cancer. *Cell* 100:57–70.
48. Vitale-Cross L, Amornphimoltham P, Fisher G, Molinolo AA, Gutkind JS (2004) Conditional expression of K-ras in an epithelial compartment that includes the stem cells is sufficient to promote squamous cell carcinogenesis. *Cancer Res* 64:8804–8807.
49. Gupta S, *et al.* (2007) Binding of ras to phosphoinositide 3-kinase p110alpha is required for ras-driven tumorigenesis in mice. *Cell* 129:957–968.
50. Cristofanelli B, *et al.* (2000) Cooperative transformation of 32D cells by the combined expression of IRS-1 and V-Ha-Ras. *Oncogene* 19:3245–3255.
51. Buchardt O, *et al.* (1986) Thermal chemistry of podophyllotoxin in ethanol and a comparison of the cytostatic activity of the thermolysis products. *J Pharm Sci* 75:1076–1080.
52. Mosmann T (1983) Rapid colorimetric assay for cellular growth and survival: Application to proliferation and cytotoxicity assays. *J Immunol Methods* 65:55–63.